Quantum conductivity in single and coupled quantum-dimensional particles of narrow-gap semiconductors

© *M.V. Gavrikov, E.G. Glukhovskoy, N.D. Zhukov*

Chernyshevsky National Research State University of Saratov,
410012 Saratov, Russia

E-mail: maks.gavrikov.96@gmail.com

An organo-modified ordered layered structure with three-dimensional close packing based on colloidal quantum-sized particles (QP) of InSb, PbS, CdSe semiconductors and Langmuir–Blodgett films has been fabricated and studied. According to the current-voltage characteristics (CVC) of single-electron transport in the model of a nanocell with a linear chain QP across the layers, the processes limiting conductivity were established: emission-injection tunneling from a probe into a nanoparticle, motion in a nanoparticle determined by the establishment of an electronic wave process in it, and tunneling through a nanogap between nanoparticles. Quasi-periodic oscillations of the current and resonant peaks of quantum conductivity are observed on the I−V characteristics, which were estimated in the quantum wire model. For an even number of layers (QP, 2, or 4), the I−V characteristics were used to determine the attenuation of size quantization and the decrease in current due to the weak interaction of nanoparticles. With an odd number (3 or 5), the nanochain acts as a single quantum thread with manifestations on the CVC similar to the cases of one QP. In this case, the motion of an electron can be considered as a one-electron charge wave.

Keywords: Nanoparticle, quantum dot, quantum-sized particle, quantum thread, quantum conductivity, electron tunneling, electronic wave process, current quantum resonance, colloidal synthesis, LB films, multilayer nanostructure, linear nanocell.

DOI: 10.61011/SC.2023.05.57149.27k

1. Introduction

Scientific and practical problems of creating hardware components for the nanoelectronics areas that have been developing in recent years continue to be relevant. The development of nanostructure manufacturing technologies has made it possible to research and develop basic elements in the form of systems of ordered quantum dots in contact with micro- and nano- electrodes [1–4]. In addition to the applied significance of these studies, they are of great scientific interest from the point of view of fundamental physical effects and the theory of the processes occurring in them [5]. Even relatively simple systems, including only a few configuratively arranged quantum dots, demonstrate a large number of quantum effects that do not always have direct analogues in bulk materials [3,6–10].

The things at issue are technological methods for producing nanostructures both on the basis of traditional microelectronics and, in particular, on the basis of new techniques of molecular electronics [11–13]. The effect of organo-modification allows the integration and multilayer formation of nanoparticles due to enhancement of the van der Waals interactions, which leads to solubilization of nanoparticles and increased affinity between them [14,15].

2. Experimental

Important for these studies is the variety of options for nanoobjects, forms and methods of their implementation.

In this study, we experimentally investigated and explained the electronic conductivity properties of linearly arranged in series from one to five semiconductor colloidal quantum-sized particles (QP) in the interelectrode nanogap of a scanning probe microscope (SPM). Experiments were carried out on random selections of a large number (more than 200) of QP samples by their colloidal synthesis, control of the shape and size of nanocrystals using a transmission electron microscope (TEM), electron-X-ray control of the composition using a scanning electron microscope, deposition on a dielectric substrate with conducting indium tin oxide (ITO) layer using Langmuir−Blodgett film (LBF) technology, measurements of current-voltage curves (IU-curves) of individual QPs and their lines in a sealed compact chamber of a probe microscope. Methodological details of the QP synthesis, control of their properties and measurements of the IU-curves are described in our studies [10,16,17]. For the research, we used QPs based on CdSe, PbS, InSb, which are the most studied semiconductors in the nanotechnology field.

The IU-curves were measured by a SOLVERNano scanning probe microscope under conditions of air-tightness of its chamber and probe-sample nanogaps of $\sim 5\,\text{nm}$ with „minus" polarity on the probe. The model of the current was as follows [9]. An electron is emitted from the probe and injected into the nanoparticle, overcoming a certain potential barrier. We call this process emission tunneling and describe it by the expression for the current $I_{\text{et}} \sim \exp(\alpha V)$. Then the electron undergoes a naturally-

Summary of key data

	m/m_0	a_0, nm	a_n, nm	$\tilde{E}_{kn}$, eV		C	p_1,	p_2,	p_3,	p_4,	p_5,
				$\tilde{E}_{k=1,n}$	$\tilde{E}_{k=2,n}$				%		
QP−CdSe	0.13	0.430	2.0−4.0	0.2−0.7	0.8−3.0	0.9	10	0	20	10	15
QP−PbS	0.080	0.593	2.5−4.5	0.2−0.8	0.8−3.2	1.1	20	15	20	10	15
QP−InSb	0.013	0.649	3.5−7.5	0.5−2.0	2.0−8.0	2.5	45	35	65	30	45

determined motion in the nanoparticle, so that its IU-curve has the form of $I_{QP} \sim V^\gamma$, and finally tunnels into the ITO electrode, overcoming the intergranular barrier, so that its IU-curve is approximated by the following formula: $I_t \sim \exp(-\beta/V)$. Each of these three processes can be a limiting factor and determine the shape of the IU-curve in its individual sections.

3. Results and discussion

The main data is reflected in the table. Parameters of semiconductors used in the study — the lattice constant a_0 and the ratio of the effective mass m to the „rest" mass of electron m_0 — are taken from the online data source [18]. The table indicates and shows: a_n — intervals of nanoparticle sizes measured on TEM images; $\tilde{E}_{kn} \sim 0.35 k^2 (m/m_0)^{-1} a_n^{-2}$ — dimensional quantization energy values obtained by solving the Schrödinger equation for linear one-electron motion, k — quantum number; energy — in eV, dimensions — in nm [9]. The $\tilde{E}_{kn}$ values are determined by the resonance of the electron wave process [19] and are calculated depending on the type of semiconductor (values of m/m_0) and QP dimensions (see the table).

The film structure was formed by the LBF method based on the amphiphilic properties of surface-active material (surfactant) molecules and their self-organization at the „gas−liquid" interface, which makes it possible to produce a densely packed molecular monolayer (ML) [20]. Arachidic acid was used as an organic matrix. The working solution was a mixture of organic matrix molecules and nanoparticles of various compositions.

To identify the state of dense packing of the monolayer, it was preliminarily studied by the compression isotherm method. For this purpose, a solution of a mixture of surfactants and nanoparticles in chloroform was applied to the surface of the aqueous subphase. After the time required for the solvent to evaporate, the layer was compressed by movable barriers. During compression, the positions of the barriers were recorded, the area occupied by the ML and the surface pressure measured by Wilhelmy plate were determined. The pressure that was required to maintain the ML at the moment of transfer was determined — in the range of $15-20 \, \mathrm{MN/m^2}$. The packing density of nanoparticles was monitored by several methods: by transmission electron microscopy, as well as by changes in the surface tension, by optical (at the Brewster angle) and scanning probe microscopy.
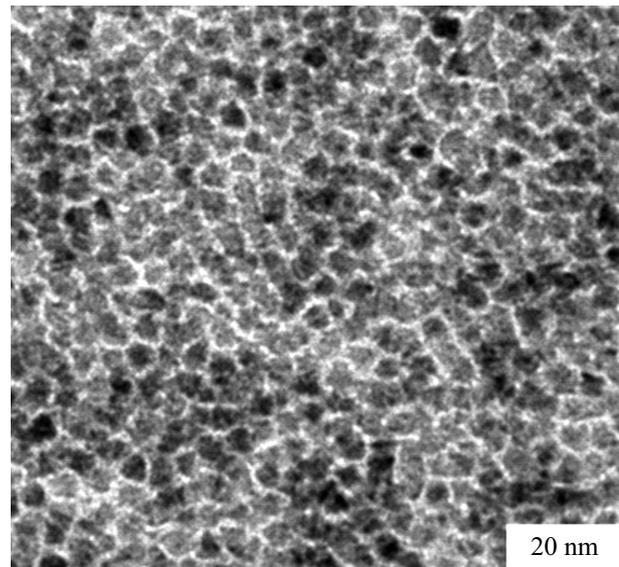

20 nm

Figure 1. Typical fragmentary TEM-image of nanoparticles on a Langmuir−Blodgett film (by the example of InSb QPs).

Figure 1 shows a typical TEM-fragment, which reflects the densely packed structure of a QP monolayer. In this case, the gap between nanoparticles generally does not exceed a tenth of their size. Thus, using the LBF method, it is possible to form an organomodified ordered layered structure with a dense packing of semiconductor colloidal nanoparticles, similar to what was done in a number of studies for nanoparticles of non-semiconductor materials [14,15].

Figure 2, a shows typical options for IU-curves, which have, among other things, features in the form of individual peaks and quasiperiodic current ripples (curves $1-4$). Curves 1 and 2 are test curves that show the absence of observable features for simple options. We believe, that the differences in types of IU-curves (curves $1-4$, Figure 2, a) are due to the degree of manifestation of the size quantization [9]: curves 1 and 4 are for a weak degree, and curves 2 and 3 are for a strong degree. At the same time, in the case of strong effect, resonant properties are manifested in the form of sharp current peaks on the IU-curve. The degree of these manifestations is determined by the type of semiconductor and the size of nanoparticles; the degree for different cases can be estimated by the following parameter: $C \sim (m/m_0)^{-1} a_n^{-2}$ [21]. The table shows values of the C
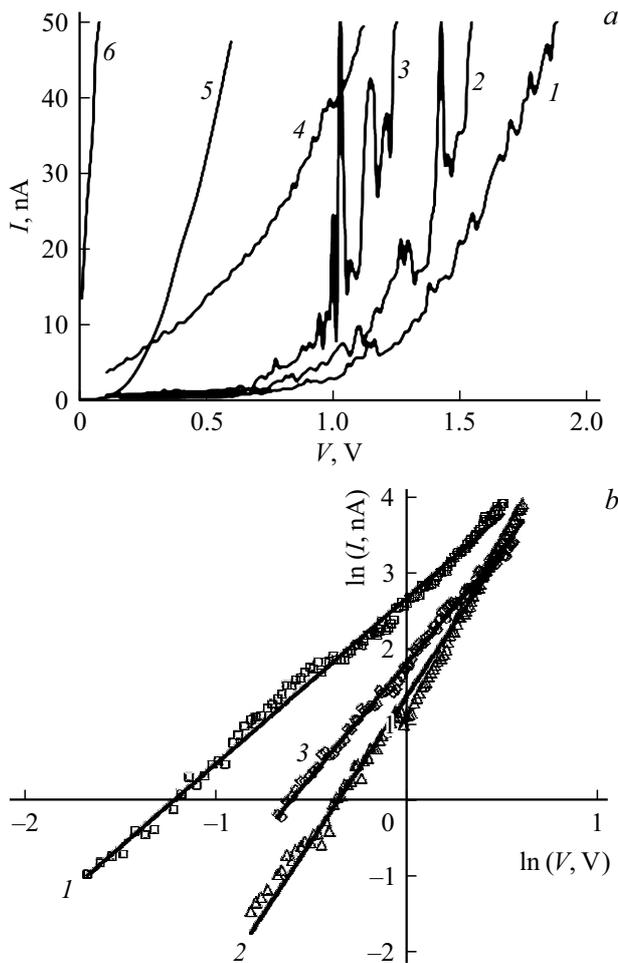
Figure 2. Typical options for the IU-curve. a — $(1-4)$: IU-curve of QP samples; 5 — IU-curve of the tunnel-emission current of InSb micron particles; 6 — IU-curve of the tunnel contact to the ITO layer. b — IU-curve in logarithmic coordinates: 1 — CdSe QPs, 2 — PbS QPs, 3 — InSb QPs.

parameter calculated for the maximum of the a_n distribution curve and the experimental data of the percentage share p_i of the number of samples with good pronounced resonance in their total number for single QPs (p_1) in one (the first) nanolayer and sequentially for several layers — $N \sim 2$, 3, 4, 5. At the same time, a trend of wave-like change in p_i is observed with minima for even N.

The IU-curves with a weak manifestation of size quantization had the form of curves of types 1 and 4 (Figure 2, a). At the same time, for the CdSe QP samples up to 80% of IU-curves were of curves of type 4. However, this type almost did not manifest for PbS QP samples and InSb QP samples. In addition, the IU-curves of type 4 were approximated by exponential functions $I_{et} \sim \exp(\alpha V)$ and $I_t \sim \exp(-\beta/V)$ with parameters $\alpha \sim 10\,\text{B}^{-1}$ and $\beta \sim 2\,\text{V}$. IU-curves of type 1 were almost not observed for CdSe QPs but were dominating for PbS QPs and especially for InSb QPs. At the same time, IU-curves were well approximated by the $I_{QP} \sim V^\gamma$ depen-

dence with the parameter $\gamma \sim 2$ for CdSe QPs and ~ 3 for PbS QPs and InSb QPs (Figure 2, b). This exponential function (with γ coefficient from 2 to 3) is explained by the model of current limitation by the space charge similar to the one-electron Coulomb blockade process [9]. In this case, the γ parameter is larger for cases with better size quantization characteristics. With an increase in the number of layers γ decreases, and this decrease is stronger for the cases of even N. For example, for InSb QPs for different $N-1$, $\gamma \sim 3.0$; 2, $\gamma \sim 2.3$; 3, $\gamma \sim 2.45$; 4, $\gamma \sim 2.25$; 5, $\gamma \sim 2.5$.

In certain voltage ranges, a typical feature of the IU-curve dependence on the number of monolayers N in the samples was observed: for their even number, the current values decreased, for an odd number they increased (Figure 3, a).

The current peaks on IU-curves (curves 2 and 3, Figure 2, a) are determined by the field energy under conditions of resonance of the electron wave process [19]. Figure 3, b shows a typical pattern of the samples conductivity N dependence on $dI/dV = G_v$ in the resonance energy zones. We interpret the resonant peaks of the one-electron conductivity of a linear QP chain as quantum conductivity in the quantum thread model [22]. Taking into account the one-electron nature of the current: $G \sim K^{-1}q^2/h \sim 4 \cdot 10^{-5}\,K^{-1} \cdot$ S, where q being electron charge, K being number of quantum steps. The ratio a_n/a_0 can be taken as the number of quantum steps in a single QP, and Na_n/a_0 can be taken as that in the entire chain [21]. In our case, $a_n/a_0 \sim 10$, and $K = Na_n/a_0 \sim (10-50)$. Then it should be: $G \sim (1-4) \cdot 10^{-6}\,$S. As can be seen from the graphs in Figure 3, $G \sim (1-2) \cdot 10^{-6}\,$S, which corresponds well to the calculation, taking into account that the differentiation interval ($\sim 30\,\text{mV}$) is almost equal to the width of the resonance peak, or in some cases it is even a little greater than this width.

The observed dependences of IU-curves can be explained with the assumption of the following physical model. For an even number N, the electronic interaction between QPs is manifested weakly. They act as if the are independent from each other. Therefore, the current through the QPs of 2 or 4 successive layers decreases as a current through resistors connected in series; the dependences show current dips for N equal to 2 or 4 (Figure 3, a). With their independent action, the characteristics of quantum conductivity are formed by simple mixing and have a more complex pattern (Figure 3, $N = 2$ and $N = 4$). For the cases of odd numbers N (1, 3 and 5) the QPs in the interlayer line act in concert as a single quantum thread, and an "ideal" pattern of quantum conductivity is observed (Figure 3, $N = 1, 3, 5$).

To explain this case of electronic interaction of nanoparticles, we assumed that a simple linear sequence of QPs should be considered as a single quantum thread with potential barriers at the nodes, i.e. the points where QPs are located. For this case, it is necessary to solve the Schrödinger equation for a single-electron transport. By neglecting the subtle effects of electrons interaction with
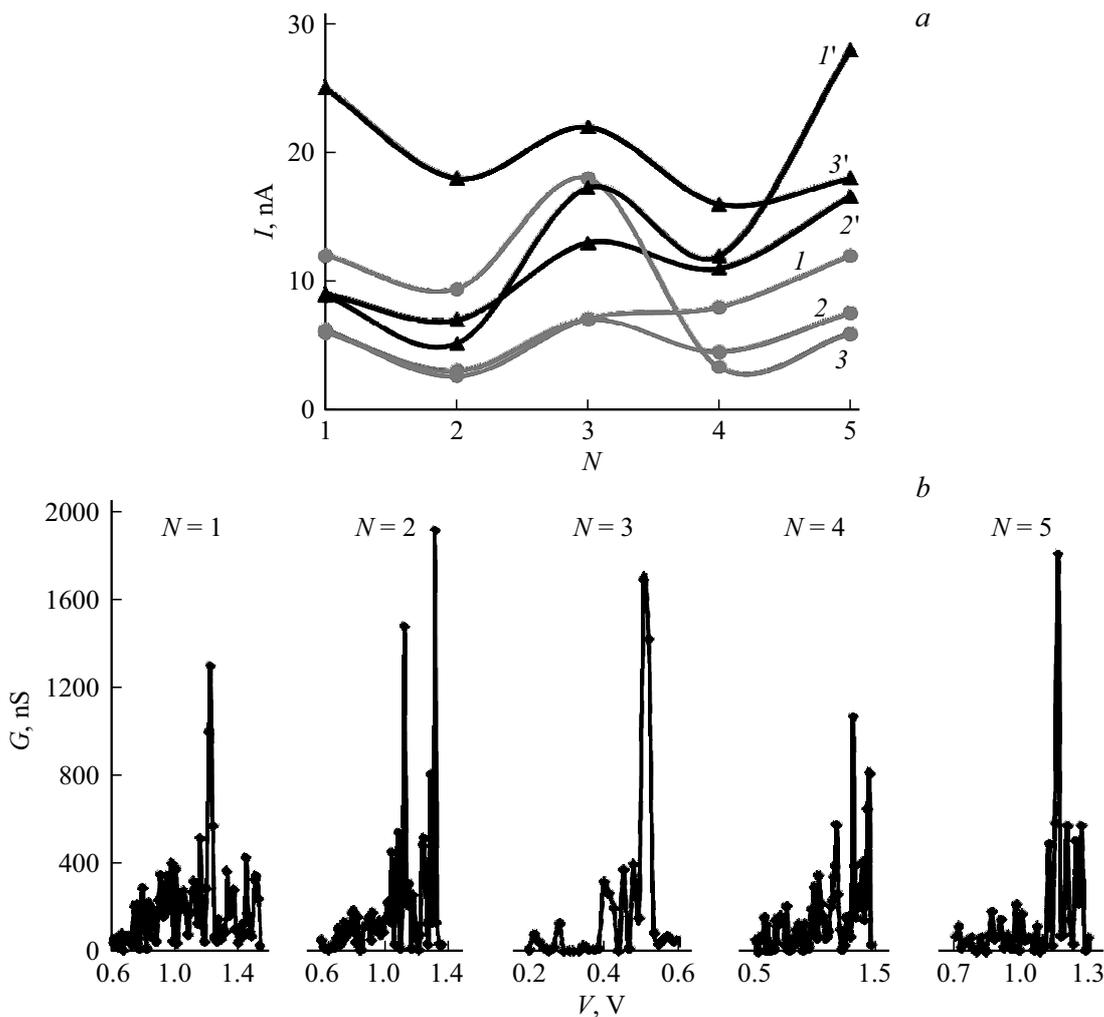
Figure 3. Dependence of IU-curves on the number of monolayers N. a — current dependences: $1, 1'$ — PQ−CdSe, $2, 2'$ — PQ−PbS, $3, 3'$ — PQ−InSb; $1, 2, 3$ — at $V \sim (0.6-0.8)$ V, $1', 2', 3'$ — at $V \sim (1-1.5)$ V. b — resonant peaks of differential conductivity (by the example of InSb QP sample).

the lattice, we can assume that resonance of the electron wave process is possible in cases of an integer number of de Broglie half-waves over the entire length of the quantum thread. For an odd number of points N the number of gaps is even, therefore this is the case when the preferable conditions for the formation of resonance are created. In this case, the electronic process itself along the quantum thread can be considered as a single-electron charge wave. It seems very interesting to create a theory of such a wave process, similar to how it was done for the macroscopic case of spatial charge waves [23].

4. Conclusion

Thus, in this study, an organomodified ordered layered (from 1 to 5 layers) nanostructure with three-dimensional dense packing based on colloidal quantum-sized particles of InSb, PbS, CdSe semiconductors and organic Langmuir−Blodgett films was fabricated and studied.

Single-electron transport has been studied in the model of a nanocell with a linear chain of nanoparticles across the layers in the interelectrode nanogap of a scanning probe microscope. Based on IU-curves, the limiting transport processes have been identified: the emission-injection tunneling from the probe into the nanoparticle, the motion in the nanoparticle determined by the establishment of an electronic wave process in it, the tunneling through the nanogap between nanoparticles. Parameters for the manifestation of size quantization are determined depending on the semiconductor option and sizes of quantum-sized particles and the number of layers in the nanostructure. The IU-curves exhibit quasi-periodic current oscillations and resonant peaks of quantum conductivity, estimated in the quantum thread model. With an odd number (3 or 5) of layers, the nanochain acts as a single quantum thread with manifestations on the IU-curve similar to those of single nanoparticle cases. In this case, the motion of the electron can be considered as a single-electron charge wave.

Funding

Conflict of interest

The authors declare that they have no conflict of interest.

References

[1] S.B. Brichkin, V.F. Razumov, Uspekhi khimii, **85** (12), 1297 (2016). (in Russian).
doi: 10.1070/RCR4656

[2] M. Alizadeh-Ghodsi, M. Pourhassan-Moghaddam, A. Zavari-Nematabad, B. Walker, N. Annabi, A. Akbarzadeh. Part. Part. Syst. Charact., **36**, 1800302 (2019).
doi: 10.1002/ppsc.201800302

[3] L. Jacak, P. Hawrylak, A. Wojs. *Quantum dots* (Berlin, Springer Science & Business Media, 2013).

[4] N.D. Zhukov, I.T. Yagudin, N.P. Aban'shin, D.S. Mosiyash. Techn. Phys. Lett., **46** (11), 1088 (2020).
doi: 10.1134/S1063785020110152

[5] V.S. Protsenko, A.A. Katanin. Phys. Rev. B, **99** (16), 165114 (2019). doi: 10.1103/PhysRevB.99.165114

[6] I. Ozfidan, A.H. Trojnar, M. Korkusinski, P. Hawrylak. Solid State Commun., **172**, 15 (2013).
doi: 10.1016/j.ssc.2013.08.011

[7] A.E. Miroshnichenko, S. Flach, Y.S. Kivshar. Rev. Mod. Phys., **82** (3), 2257 (2010). doi: 10.1103/RevModPhys.82.2257

[8] R. Zitko, J. Bonca. Phys. Rev. B, **76** (24), 241305 (2007).
doi: 10.1103/PhysRevB.76.241305

[9] N.D. Zhukov, M.V. Gavrikov. Pisma ZhTF, **48** (8), 18 (2022). (in Russian). doi: 10.21883/PJTF.2022.08.52361.19090

[10] S.A. Sergeev, M.V. Gavrikov, N.D. Zhukov, Pisma ZhTF, **48** (9), 32 (2022), doi: 10.21883/PJTF.2022.09.52448.19115 (in Russian)

[11] I.I. Abramov, Nano- i mikrosistemnaya tekhnika, **3**, 57 (2007). (in Russian).

[12] A.J. Al-Alwani, K.I. Kosolapova, A.S. Chumakov, V.O. Lykyanova, I.A. Gorbachev, A.V. Kazak, A.I. Smirnova, S.N. Shtykov, N.V. Usol'tseva, E.G. Glukhovskoy. BioNanoSci., **8** (4), 1081 (2018). doi: 10.1007/s12668-018-0537-0

[13] O.A. Shinkarenko, R.A. Safonov, A.S. Kolesnikova, A.J. KAl-Alwani, M.V. Pozharov, E.G. Glukhovskoy. Appl. Surf. Sci., **424**, 177 (2017). doi: 10.1016/j.apsusc.2017.02.256

[14] M. Iizuka, Yu. Shidara, A. Fujimori. Graduate School of Sci. and Eng., Saitama University, 225, MATEC Web Conf. (Japan), **97**, 1 (2017). doi: 10.1051/matecconf/20179801001

[15] T. Yamamoto, Y. Umemura, O. Sato, Y. Einaga. J. Am. Chem. Soc., **127**, 16065 (2005). doi: 10.1021/ja053131e

[16] N.D. Zhukov, T.D. Smirnova, A.A. Khazanov, O.Yu. Tsvetkova, S.N. Shtykov, FTP, **55** (12), 1203 (2021). (in Russian). doi: 10.21883/FTP.2021.12.51706.9704

[17] N.D. Zhukov, M.V. Gavrikov, Mezhdunar. nauch.-issled. zhurn., **8** (110), 19 (2021), doi: 10.23670/IRJ.2021.110.8.004 (in Russian).

[18] http://xumuk.ru/encyklopedia

[19] G.F. Glinsky. Pisma ZhTF, **44** (6), 17 (2018).
doi: 10.21883/PJTF.2018.06.45763.17113 (in Russian)

[20] I.A. Gorbachev, S.N. Shtykov, G. Brezesinski, E.G. Glukhovskoy. SpringerScience+BusinessMediaNewYork, **7**, 686 (2017). doi: 10.1007/s12668-017-0404-4

[21] N.D. Zhukov, M.V. Gavrikov, S.N. Shtykov, FTP, **56** (6), 552 (2022). doi: 10.21883/FTP.2022.06.52588.9809 (in Russian).

[22] N.T. Bagraev, A.D. Buravlev, L.E. Klyachkin, A.M. Malyarenko, V. Gelhoff, V.K. Ivanov, I.A. Shelykh, FTP, **36** (4), 462 (2002). (in Russian).

[23] V.V. Bryksin, P. Kleinert, M.P. Petrov. FTT **45**, 11, (1946). (in Russian).

Translated by Y.Alekseev